'90 KACC 1990. 10. 26~27

# CONTROL OF SERVOMOTOR FOR HOSPITAL MOBILE ROBOTS

**Ichiro Kimura, Keigo Watanabe, Sang-Ho Jin and Satoru Kaneko**

Department of Mechanical Engineering, Faculty of Science and Engineering,
Saga University, Honjomachi-1, Saga 840, Japan.

**Abstract**

A d.c. servomotor with pulse encoder is used to improve the movement of a hospital mobile robot along the desired line. We can achieve an improved movement of the robot by applying a PLL control. It is then shown that we can also reduce 42% of the power dissipation by the use of a PWM control. Furthermore, some simulation studies are presented to illustrate the design of PI control and optimal regulator for the control of the d.c. servomotor.

## 1. Introduction

An automated guided vehicle can be considered as an automated mobile conveyer designed to transport materials [1, 2]. In particular, the hospital mobile robot (HMR)can guide patients and transport files of medical reports, blood and urea to be analyzed. The HMR which has been developed recently [3] was guided by a strip of aluminium tape. The two drive wheels of the HMR were separately driven by two d.c. motors with constant current. The control method of the motors is not economical enough because we need a large power to drive the d.c. motors. Furthermore, it is not easy to control the robot's position in turning movements.

In this paper, two d.c. servomotors with a pulse encoder are used to improve the movement of the robot along the desired line. First, an improved movement is obtaind by applying a PLL (Phase Locked Loop) control, and it is then shown that we can reduce 42% of the power dissipation by making use of a PWM (Pulse Width Modulation) control. Furthermore, some simulation studies are performed to illustrate the designs of PI control and optimal regulator for the control of the d.c. servomotors. We finally discuss the application of such a controller to the HMR.

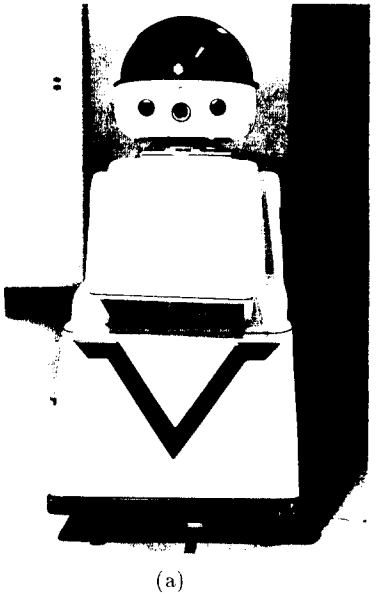

(a)

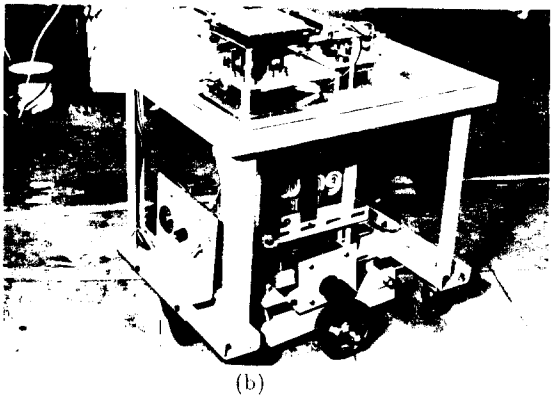

(b)

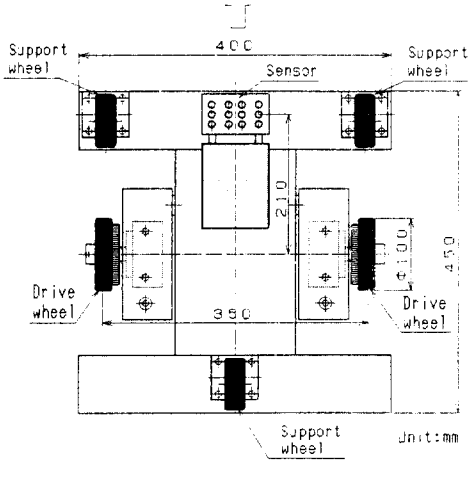


(c)

Fig. 1 Design of experimental hospital mobile robot.

## 2. Construction of Systems

### *2.1 Specification and Traveling method*

Fig. 1 shows the experimental HMR: (a) Outlook; (b) Mechanism; and (c) Bottom view. The specification of experimental HMR is as follows: height is 99cm; width is 49cm; weight is 35 kg; and drive motor is a d.c. servomotor (Type: DME44SM8H18A made by Japan Servo Co., Ltd.) with a magnet type pulse encoder (12 p/rev). The output of the drive motor torque is 5.5 kgcm and the gear has reduction ratio 1/32.

The block diagram of the system for the experimental HMR developed here is shown in Fig. 2. The revolutions of d.c. servomotors to right- and left-side wheels are controlled by using a Z-80 single board computer (SM-B-80TE). The guide system has sensors for detecting light reflected from an alminium tape of 13 mm width on the floor. The infrared ray sensor used here (see Fig. 3) can detect the light of 5mm width radiated from a slit of 2mm width. As can be seen from Fig. 3, the global sensor system consists of four sets of a local infrared ray sensor, where the local sensor is further composed of one emitter and two detectors connected in parallel. It is assumed that the state of each local sensor takes 1 when the signal of the associated detector is in high level (H) and similarly the state of each local sensor takes 0 when the signal of the associated detector is in low level (L). The global sensor system then transmit a set of four states to the I/O port. When both states of second and third local sensors located inside take 1, i.e., the state of the global sensor system takes (0110), the computer commands the d.c. motors to do the forward revolution. If the state of the global sensor system takes (0010), the right-side motor is stopped and the left-side motor is driven until the state of third local sensor takes 1. Conversely, if the state of global sensor system takes (0100), the motor is driven to the opposite direction. The change of direction for the HMR is perfomed as follows: the clockwise rotation of 90 degrees is made when the state of the fourth local sensor takes 1; the counterclockwise rotation of 90 degrees is made when the state of the first local sensor takes 1; and a round of rotation is made when all the states of local sensors take 1, i.e., the state of the global sensor system takes (1111). The controlled angle for the left- and right-side wheels is $\tan^{-1} 2.5/210 \simeq 0.7$(deg).

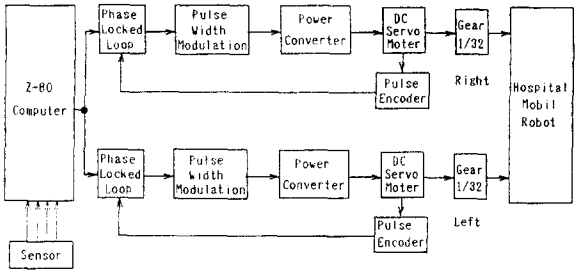


Fig. 2 Block diagram of the robot drive equipment.

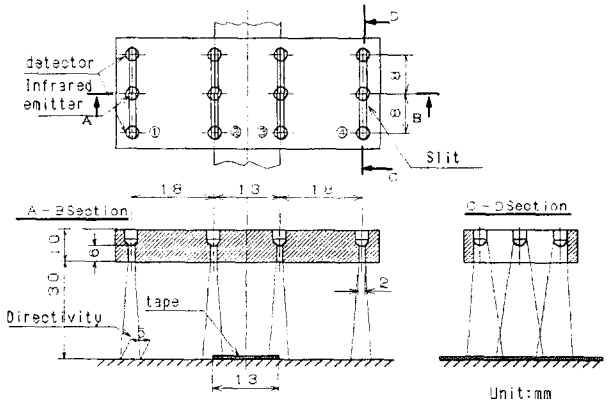


Fig. 3 Sensors for travelling.

### *2.2 PLL Control*

The number of revolution for the motor is controlled by using a PLL circuit. This PLL control selects a desired revolution per minute among three specified revolutions: 3800 rpm; 2300 rpm; and 1150 rpm, which correspond to three frequencies, i.e., 3.07 MHz, 1.535 MHz and 0.7675 MHz, respectively. The Z-80 computer selects one frequency generated by using the natural frequency 6.14 MHz of a crystal transmitter. In the PLL circuit, comparing a specified frequency with an actual one feeded back from the PE and simultaneously comparing a specified phase with the actual one, we have two compared values. Furthermore, transmitting frequency and phase to the D/A converter and adding them, we have a voltage required for the PWM.

Since we would like to apply the experimental HMR to the pediatrics, the velocity of HMR was set to 370 mm/sec (i.e., 2300 rpm). The number of revolution for the idling case was measured. The result is tabulated in Table 1. When traveling on the floor, it was found that a control angle of about 0.9 (deg) was reguired for a traveling distance of about 1.3 (m), whereas a control angle of about 1.5 (deg) was reguired in the earlier study [3]

Table 1 Measured number of revolution, where the specified number of revolution is 2300 rpm.

| NO | 1 | 2 | 3 | 4 | 5 | 6 | 7 | 8 | 9 | 10 |
|---|---|---|---|---|---|---|---|---|---|---|
| RPM | 2310 | 2335 | 2320 | 2305 | 2300 | 2340 | 2350 | 2320 | 2320 | 2320 |

*2.3 PWM Driving*

The HMR developed earlier had a driving circuit for one wheel, where two d.c. motors were separately driven by a constant current. Because of such a linear current, it was required for the driving circuit to consume a large amount of power. The present driving circuit is controlled in a switching way by using a pulse signal (see Fig. 4) generated from comparing the saw wave (27 KHz) (see Fig. 5) of PWM with the voltage from the PLL. We can reduce 42% of driving power by applying the present PWM, compared with the earlier driving circuit. This is confirmed form a fact that the present power demand is 9.8 W, whereas the earlier one is 16.8 W.

## 3. Control Design using Simulations

In this section, we shall describe the simulation results for designing an optimal controller to control the d.c. servomotors.

*3.1 Derivation of Transfer Function*

Fig. 6 shows the step responses in the idling and loading cases. From the latter case, we had a damping factor $\zeta = 1.2$, a natural frequency $\omega = 10$ (rad/s) and a settling time 1.0 (s). As a result, the transfer function is represented by

$$G(s) = \frac{100}{s^2 + 24s + 100}$$

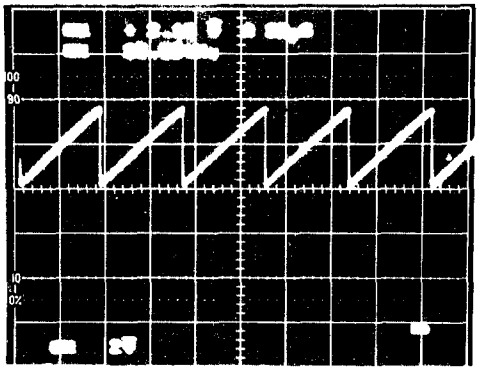

Fig. 4 Basic saw wave of PWM

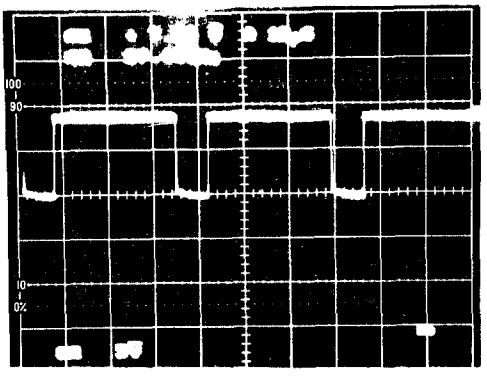

Fig. 5 Output wave of PWM.

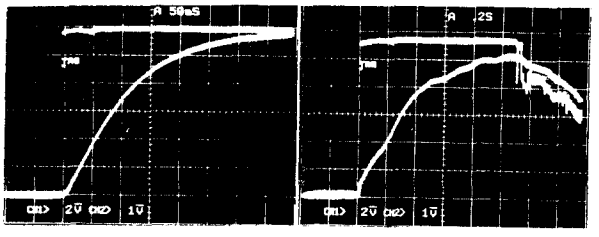

(a) Idling (b) Loading : Weight + 11 kg

Fig. 6 Step response.

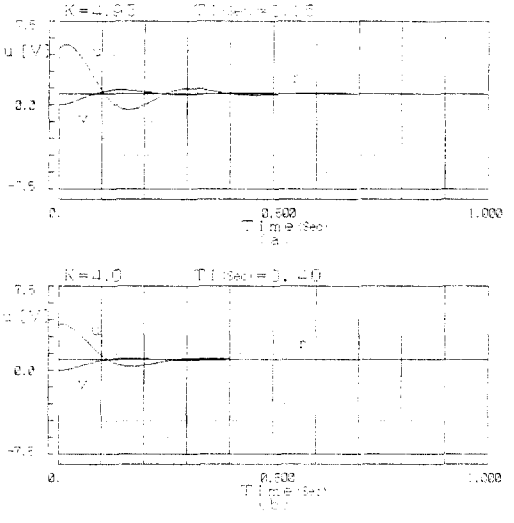

Fig. 7 Simulation results of PI control.

*3.2 Simulation results for PI controllers*

The P gain and I time were obtained by applying the Ziegler-Nichols ultimate sensitivity method. Fig. 7(a) depicts the result for a case when the proportional gain $K$ is 4.95 and the integral time $T_i = 0.15$(s). It is seen from this figure that the corresponding settling time is 0.68(s). Fig. 7(b) shows the result for a case when the proportional gain $K$ is 4.0 and the integral time $T_i = 0.40$(s). From this figure, we find that the corresponding settling time is 0.40(s). Comparing of these figures, the parameters used in Fig. 7(b) can be selected as candidate ones for a better PI controller.

*3.3 Simulation results for optimal regulators*

Transforming the transfer function obtained above to the representation of state-space, it follows that

$$\dot{x} = Ax(t) + Bu(t) \tag{1}$$

$$y = Cx(t) \tag{2}$$

where

$$A = \begin{bmatrix} 0.0 & 1.0 \\ -100 & -24 \end{bmatrix} \quad B = \begin{bmatrix} 0.0 \\ 1.0 \end{bmatrix} \quad C = [1 \quad 0]$$

We want to look for a control $u(t)$ which minimizes the following cost functional:

$$J(u) = \int_0^\infty \left\{ y^T(t) Q y(t) + u^T(t) R u(t) \right\} dt \qquad (3)$$

If $(A, B)$ is stabilizable and $(C, A)$ is detectable, then there exists an $n \times n$ positive semidefinite matrix satisfying

$$PA + A^T P - PBR^{-1}B^T P + C^T Q C = 0 \qquad (4)$$

Using this matrix, we obtain an optimal input $u_o(t)$ that minimizes $J(u)$ so that

$$u_o(t) = Kx(t) \qquad (5)$$

$$K = -R^{-1}B^T P \qquad (6)$$

Fig. 8 shows the block diagram of the optimal regulator. The simulation results are presented in Figs. 9(a) and 9(b). Fig. 9(a) is for a case when weights $Q = 50, R = 1$, control gain vector $K = [-6.140 \quad -0.185]$ and initial state $x(0) = [0.17 \quad 0]^T$, where the poles of closed-loop system $(A + BK)$ are located at $-21.2 \pm j16.2$. It is seen from this figure that the settling time is about 0.25 (s). Fig. 9(b) is also for a case when weights $Q = 100, R = 1$, control gain vector $K = [-9.050 \quad -0.248]$ and initial state $x(0) = [0.17 \quad 0]^T$, where the poles of closed-loop system are located at $-24.4 \pm j20.2$.

*3.4 Simulation results for observer-based regulators*

In order to realize the above regulator, it is required to estimate the first state-variable, because the second state-variable can not be measured directly. Since the pair $(C, A)$ is observable, we may construct a reduced-order observer. Fig. 10 shows the block diagram of the minimal-order observer. The simulation results, for a case when this reduced-order observer is incorporated with the former regulator described in 3.3, are presented in Figs. 11(a) and 11(b). Fig. 11(a) is for a case when the pole of reduced-order observer is $-25+j5$, initial state $\hat{x}(0) = [0.17 \quad 0]^T$, and the observer gain $G = 13.8$. Fig. 11(b) is for a case when the pole of reduced-order observer is $-100 + j5$, initial state $\hat{x}(0) = [0.17 \quad 0]^T$, and the observer gain $G = -8740$. From these figures, we see that the former controller is recommendable for a practical case, because it gives a faster settling time (about 0.17 (s)) and has a less control value, compared with the latter controller.

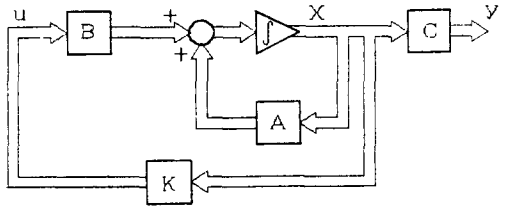


Fig. 8 Block diagram of optimal regulator.

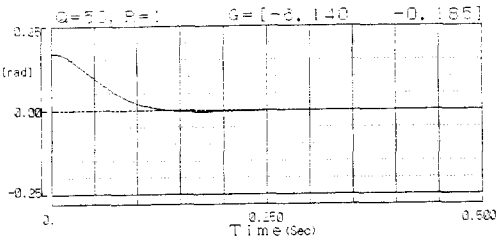


Response of $y$

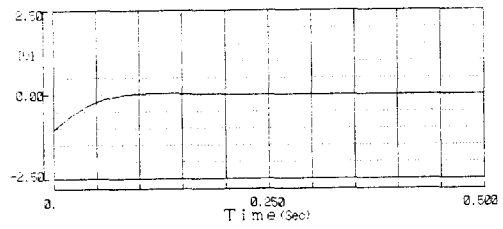


Control $u$

(a)

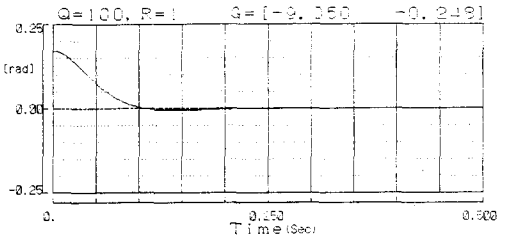


Response of $y$

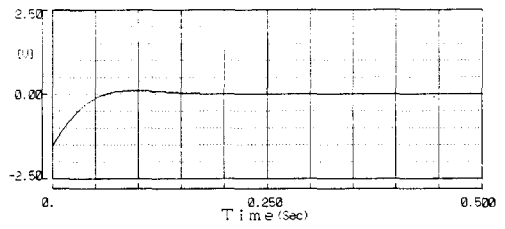


Control $u$

(b)

Fig. 9 Simulation results of optimal regulator with complete state information.

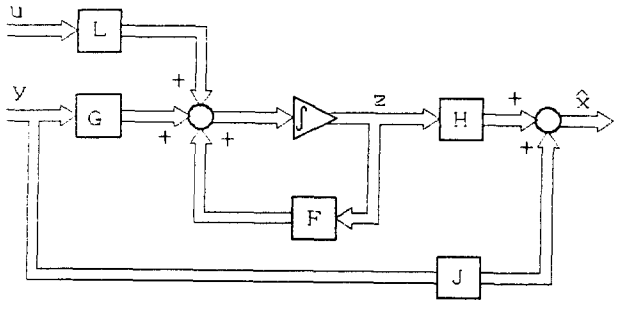


Fig. 10 Block diagram of minimal-order observer.

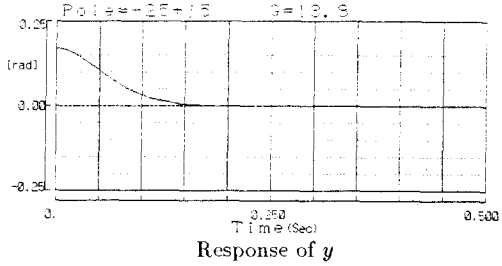


Response of $y$

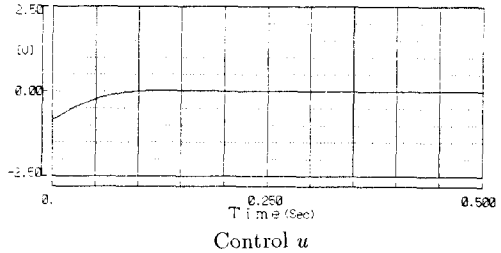


Control $u$

(a)

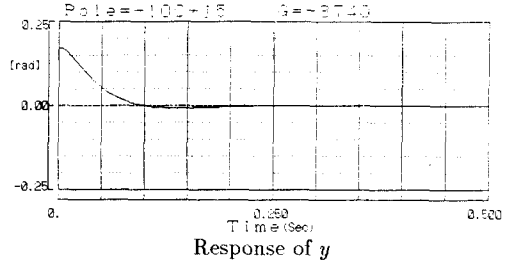


Response of $y$

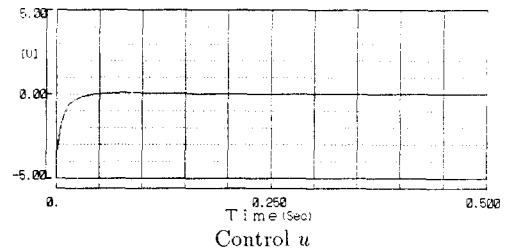


Control $u$

(b)

Fig. 11 Simulation results of optimal regulator with incomplete state information.

## 4. Conclusions

We have developed a hospital mobile robot (HMR) controlled by the phase locked-loop circuit, where the d.c. motors used in an earlier experiment [3] have been replaced by the d.c. servomotors. From some experimental results, we can conclude that the present HMR has a better performance than that for an earlier developed HMR. In addition, we have reduced 42% of power dissipation by using the PWM control. We may further improve the performance of HMR by applying a better pulse encoder, because the magnet type pulse enceder used here has insufficient performance.

We have determined some parameters reguired for PI controller, optimal regulator and reduced-order observer to control the d.c. servomotor by using several simulations. Applying these parameters, we will be able to develop an analog controller or a computer-based controller in the mean time.

## References

[1] E. Sung, Ng K. Loon, and Y. C. Yin: "Parallel Linkage Steering for an Automated Guided Vehicle", *IEEE Control Systems Magazine*, October, pp.3-8, 1989.

[2] K. Komoriya, K. Tanie, "Trajectory Control of a Wheel-type Mobile Robot Using B-Spline Curve", *Journal of the Robotics Society of Japan*, Vol.8, No.2, pp.1-11, 1990 (in Japanese).

[3] I. Kimura and J. Tadano, "Control of Guide and Carry Robots for Hospital Use", Trans. of SICE, Vol.25, No.7, pp.808-814, 1989 (in Japanese).